International Journal of Thermal Sciences 49 (2010) 272–280

Contents lists available at ScienceDirect

International Journal of Thermal Sciences

journal homepage: www.elsevier.com/locate/ijts

# Flow and thermal characteristics of offset branching network

Xiang-Qi Wang [a], Peng Xu [a,b], Arun S. Mujumdar [a,*], Christopher Yap [a]

[a] Department of Mechanical Engineering, National University of Singapore, Singapore 117576, Singapore
[b] School of Physics, Huazhong University of Science and Technology, Wuhan 430074, Hubei, PR China

ARTICLE INFO

*Article history:*
Received 11 June 2007
Received in revised form
21 July 2009
Accepted 22 July 2009
Available online 12 August 2009

*Keywords:*
Tree-like network
Leaf-like network
Offset
Symmetric

ABSTRACT

Inspired by natural branching systems such as tree canopy, leaves, plant root, river basins, mammalian circulatory and respiratory systems, branching networks have been suggested for electronic component cooling. However, previous studies of tree-like branching networks have focused on symmetric structures although most natural tree-like branching systems are asymmetric. Furthermore, leaf-like branching networks have been rarely used and discussed. A three-dimensional model was formulated to compare the flow and heat transfer characteristics of symmetric/asymmetric tree-like branching networks and symmetric/asymmetric (offset) leaf-like branching networks. Results show that the influence of the asymmetry is very small for tree-like branching network at low branching number. Offset in leaf-like branching networks can reduce pressure drop significantly while maintaining maximum temperature difference between the inlet and outlet of the flowing fluid.



## 1. Introduction

The efficient transport characteristics of natural branching systems/networks such as tree canopy, leaves, plant root, river basins, mammalian circulatory and respiratory systems can provide useful hints for optimal solutions of many engineering problems, which have fascinated researchers in physics, chemistry, biology, physiology, engineering and geology for ages and been applied in microelectronic cooling, flow-field designs in fuel cell, fluid distributor, micro-fluidic manifolds in lab-on-a-chip systems etc [1–9]. The introduction of branching networks into micro-channel cooling technique has stimulate this field and attracted increased interest in studying heat and mass transfer properties in branching micro-channels [2–4,10–16].

Since Tuckerman and Pease [17] first incorporated micro-channels in heat sinks for electronic component cooling, numerous investigators have examined thermal and flow characteristics of microchannels, which display some attractive advantages such as increased heat transfer coefficient and increased area/volume rations. However, the conventional parallel microchannels do have some drawbacks. The convective heat transfer in microchannel flows is significantly enhanced, but it is achieved at the expense of increased pumping power. Another disadvantage of microchannel heat sinks is the nonuniform temperature distribution obtained under constant heat flux conditions. To address the issues of non-uniformity of the wall temperature, Bau [18] proposed a tapered channel which can yield lower cross-sectional resistance at the channel exit than that at the inlet. It is desirable to increase temperature uniformity while decreasing the pressure drop. The basic concepts involve reduction of the wall temperature and pressure drop using multi-scale branching flow networks similar to those found in various biological systems.

The constructal theory, proposed by Bejan [2], used the optimization approach to minimize pumping power at the minimal volume of the heat exchanger. The macroscopic branching structures can be deduced by constructal theory, and the results indicate that these structures can increase total convective heat transfer rate and offer the minimal resistance to flow and minimal pressure drop in fluid, compared with the conventional parallel channels. Following Bejan's constructal theory, many researchers have proposed various designs of constructal branching flow networks. Zimparov et al. [19,20] optimized the thermodynamic performance of simple T- and Y-shaped flow systems under fixed temperature of the channel walls. Biserni et al. [21] used constructal theory to optimize the geometry of H-shaped cavity. They demonstrated that the geometrical complexity should evolve gradually for the global flow system performance to improve. Bello-Ochende et al. [22–24] presented the geometric optimization of a three-dimensional microchannel heat sink. They found that the degrees of freedom have a strong effect on the peak temperature.

Several researchers have investigated heat and mass transfer characteristics in deterministic branching networks, which can

* Corresponding author. Tel.: +65 6874 4623; fax: +65 6779 1459.
*E-mail address:* mpeasm@nus.edu.sg (A.S. Mujumdar).

1290-0729/$ – see front matter © 2009 Elsevier Masson SAS. All rights reserved.
doi:10.1016/j.ijthermalsci.2009.07.019

**Nomenclature**

| | |
|---|---|
| $A$ | area, $m^2$ |
| AC | constant in Eq. (1) |
| $c_p$ | specific heat capacity, J/kg K |
| $d$ | hydraulic diameter of the channel segment, mm |
| $h$ | height of the channel, mm |
| $h'$ | heat transfer coefficient, $W/m^2$ K |
| $H$ | height of the heat sink |
| $k$ | thermal conductivity, W/m K |
| $l$ | length of channel segment, mm |
| $L$ | length of rectangular heat sink |
| $\dot{m}$ | mass flow rate, g/s |
| $m$ | total number of branching levels beyond 0th |
| $n$ | number of bifurcations per channel segment |
| $p$ | pressure, pa |
| $q''_0$ | heat flux, $W/cm^2$ |
| $R$ | radius of disk-shaped heat sink |
| $T$ | temperature, K |
| $V$ | velocity, m/s |
| $w$ | width of channel segment, mm |
| $W$ | width of rectangular heat sink |
| $x, y, z$ | coordinates, m |

*Greek symbols*

| | |
|---|---|
| $\Delta$ | Euclidean number of system |
| $\lambda$ | thermal conductivity, W/m K |
| $\mu$ | dynamic viscosity, pa s |
| $\rho$ | density, $kg/m^3$ |
| $\theta$ | branching angle |

*Subscripts*

| | |
|---|---|
| c | chip |
| in | inlet |
| $k$ | branching level, 0,1,2,… |
| max | maximum |
| s | heat sink |
| t | branching network |
| tot | total |

provide direct instructions for industrial applications in electronic cooling. The structures of the branching network in which each successive daughter branch has a diameter smaller than that from which it originates, are deterministic, and the branching ratios are kept as constants according to Murray's law and West et al.'s results [1,25]. Pence et al. [3,10,11] have proposed one-dimensional model for fractal-like branching network and computed the pressure and temperature distributions, their results indicate robustness compared to conventional parallel straight networks. Chen and Cheng [4,13] studied a fractal-like branching network of rectangular shape theoretically and experimentally, they argued that the fractal-like branching network can increase the total convective heat transfer and reduce the total pressure drop in the fluid compared with the conventional parallel channels. Wang et al. [14–16] numerically investigated a three dimensional physical model where the tree-like branching micro-channel networks are embedded between the heated chip and the heat sink. Their results documented decreased gradient of performance improvement obtained by increasing the complexity of channel geometries. More complex networks do not necessarily provide better thermal performance. Fabrication costs also mount with complexity of the network.

So far most investigators have mainly focused on the study of symmetric tree-like networks with several branches. When one examines in detail the structure of branching systems, it is observed that asymmetric geometries are also found in nature. Thus, the present work aims at determining whether asymmetric branching provides any practical advantage over the symmetric ones, especially for electronic cooling. The second aim is to examine the so called leaf-like branching network. Fig. 1 shows two types of leaves displaying symmetric and asymmetric branching structures. Unlike the tree-like branching networks, which are widely studied for application in electronic cooling, leaf-like branching networks have rarely been investigated. The present study was undertaken to obtain further understanding of such symmetric and offset leaf-like networks and compare them with tree-like branching networks. The "offset" here refers to the separation distance between branches; branching does not occur symmetrically at the same location along the main channel. Fewer assumptions are made in this analysis to provide better predictions. In many previous work, the effect of bifurcation on heat transfer and pressure drop was neglected; it was assumed for simplicity that the laminar flow is fully developed both thermally and hydrodynamically. Such an assumption is inappropriate if the length-to-diameter ratio is not large enough and the Reynolds number is rather large. The Navier Stokes and energy equations are solved numerically in three dimensions in conjunction with a constant heat flux boundary condition at the channel walls.

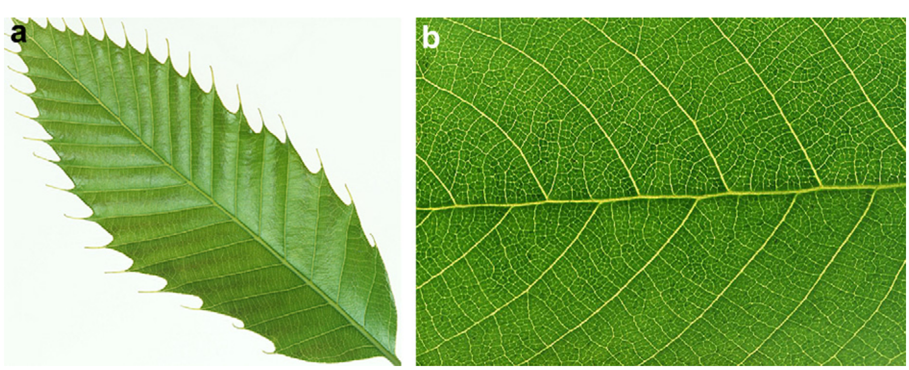


**Fig. 1.** Two types of leaves: (a) Symmetric leaf structure; (b) Asymmetric leaf structure.

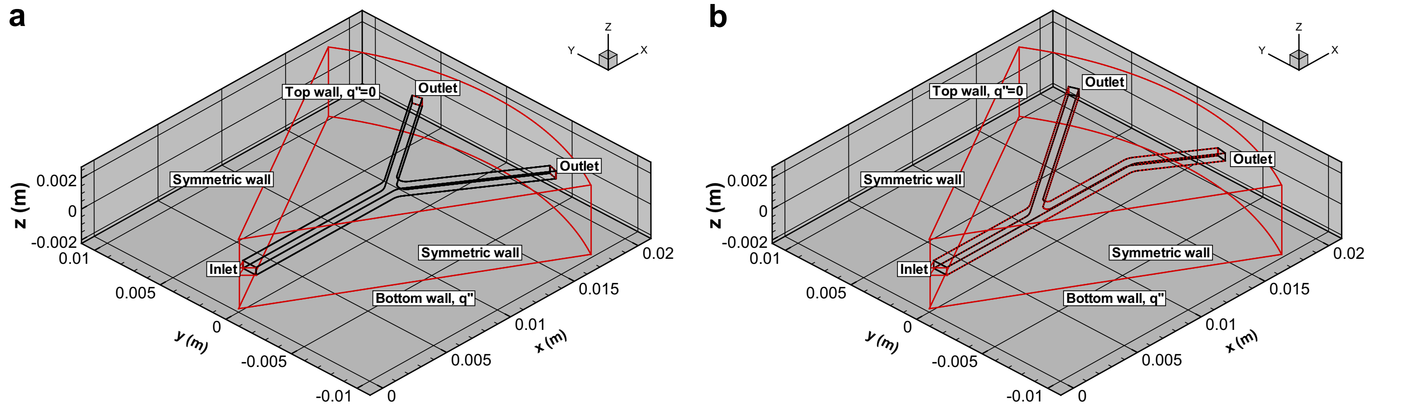


**Fig. 2.** Physical models of two tree-like networks ($m = 1$): (a) Symmetric; (b) Offset, asymmetric.

## 2. Model and analysis

Heat sinks with different patterns can be generated by simply altering variables such as the number of inlet branches, the branching angle, and branch levels, etc. The designs of tree-shaped flow patterns can be characterized by the following scaling laws [1,3]:

$$d_{k+1}/d_k = n^{-1/\mathrm{AC}}, \quad k = 1, \ldots, m \tag{1}$$

$$l_{k+1}/l_k = n^{-1/\Delta}, \quad k = 1, \ldots, m \tag{2}$$

where $d_k$ and $l_k$ represent the hydraulic diameter and length of the channel segment in level $k$, respectively. The number of branches into which a single channel bifurcates is denoted by $n$, and $\Delta$ is the Euclidean dimension the system. For the planar system, $\Delta = 2$ ($\Delta = 3$ if it is volume filling), to minimize the pumping power, following Murray's law [25], AC = 3 for the bifurcating channel configurations ($n = 2$). It is noted that the channel height h is fixed at a constant considering the ease of fabrication for future experimental validation. However, as noted by Pence and Enfield [11], there is a major problem in going to high branching levels when using a hydraulic diameter as a branching ratio to characterize rectangular channels, viz. the width of channel segments would decrease rather quickly with increased branch levels. To alleviate it, a fixed width ratio was employed instead of the hydraulic diameter,

$$w_{k+1}/w_k = n^{-1/3} \tag{3}$$

where $w_k$ denotes the width of the channel segment at level $k$. It should be pointed out that this optimal branching ratios (Eqs. (1)–(3)) are only valid for laminar flow in branching systems. The scaling exponents for electrical conduit, diffusion and turbulent flow [26–28] are different from those for laminar flow. Recently, Zhang et al. [29] presented the optimal step in the sizes of two successive cross-sectional areas is closely approximated by $2^{-2/3}$ even then the cross section is not square or round. However, there are no clear results about the optimal branching ratios for heat convection which is the combination of heat conduction and mass flow. Therefore, Eq. (3) will be used in the following simulations for approximation.

To make the comparison reasonable, several geometric parameters have to be fixed during the network design. In the current study, aside from Eqs. (1) and (3), the following two geometric constraints are employed:

- The total convective area ($A_{\mathrm{tot}}$) for each flow network is fixed, $A_{\mathrm{tot}} = \sum_{k=0}^{m} 2n^k(w_k + h_k)l_k$;
- The inlet cross-section area ($A_{\mathrm{in}}$) at level $k = 0$ is fixed for different networks.

This paper consists of two parts. First, a comparison is made between simple symmetric and asymmetric networks ($m = 1$). Then an analysis of the more complicated networks ($m = 3$ for the tree-like network) is carried out. The typical configuration tested here is a three-dimensional heat sink with embedded tree-like channel networks, as shown in Fig. 2(a) and (b). As compared with the symmetric structure shown in Fig. 2(a), Fig. 2(b) shows the asymmetric structure in which two sub-channels ($k = 1$) are placed in offset positions. It is noted that the channel dimensions of the two tree-like networks are shown in Table 1. For generation of the symmetric physical model, to save the computational time, only 1/6 of the disk-shaped heat sinks ($R = 20$ mm and $H = 4.5$ mm) is considered here due to symmetry. The bifurcation angle is set at 74.9° following Wechsatol et al. [30].

For more complex networks, symmetric/offset leaf-like networks were designed. Similar to the geometry discussed previously, the channel networks are embedded between the heated chip and the heat sink. Two-dimensional views of the physical models are shown in Fig. 3: tree-like network ($m = 3$), symmetric leaf-like network, and offset leaf-like network. The heat sink used here is a rectangular one with $L = 20$ mm, $W = 9$ mm, and $H = 4.5$ mm ($H = h_s + h_t + h_c$). For design of the tree-like network, Eqs. (1) and (3) were followed. For the leaf-like designs, the width of the main channel (or central channel) decreases from $w_0$ to $w_3$ linearly from inlet to outlet, and the width of the side channel segments is designed to be the same as the width at $k = 3$ in the tree-shaped channel. The bifurcation angle between the main channel and side channel is fixed at 60°. Furthermore, the total convective heat transfer areas for the three networks are kept the same for comparison. The detailed channel dimensions of the three nets simulated are shown in Table 2.

As shown in Fig. 2, the bottom wall is subjected to a constant heat flux ($q_0''$). The channel is cooled by a single-phase fluid at $T_0$, which is forced into the channel at a specified flow ($\dot{m}$). The coolant is modeled as a Newtonian fluid with the temperature-dependent

**Table 1**
Channel dimensions of tree-like networks ($m = 1$). $R = 20$.(unit: mm).

| Case | $h_t$ | $l_0$ | $w_0$ | $d_0$ | $l_1$ | $w_1$ | $d_1$ | $\theta$ (°) | $A_{\mathrm{in}}$ | $A_{\mathrm{tot}}$ |
|---|---|---|---|---|---|---|---|---|---|---|
| Symmetric | 0.5 | 11.7 | 1.0 | 1.5 | 9.2 | 0.8 | 0.6 | 74.9 | 0.5 | 83 |
| Asymmetric | 0.5 | 8.14 | 1.0 | 1.5 | 10.73 + 9.61 | 0.8 | 0.6 | 74.9 | 0.5 | 83 |

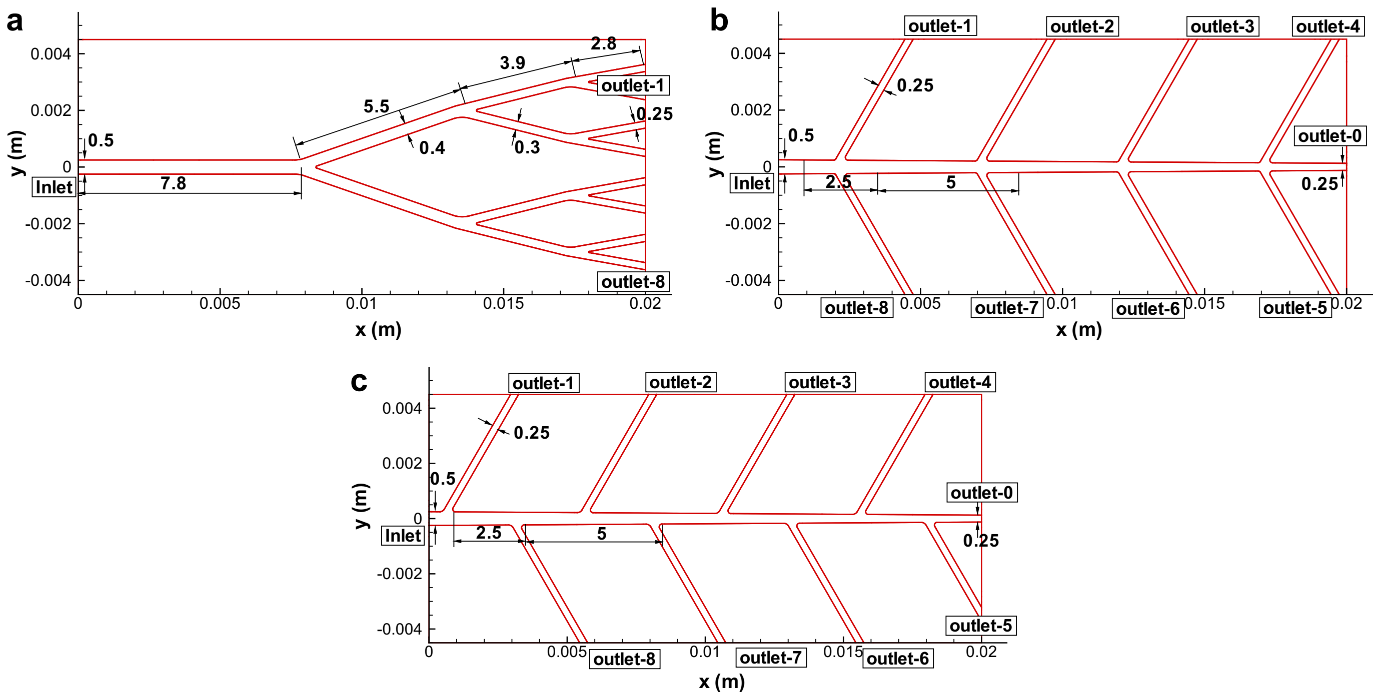


**Fig. 3.** Physical models of three different networks ($m = 3$): (a) Symmetric tree-like network; (b) Symmetric leaf-like network; (c) Asymmetric leaf-like network.

properties given in Table 3. Properties of the solid (silicon) are assumed constant at $T = 310$ K, as shown in Table 3. The numerical simulations were conducted using Fluent 6.2 which is a CFD code based on the finite volume method. A steady, incompressible and laminar flow is considered. The equations in vector notation for the steady-state conservation of mass, momentum and energy are as follows:

$$\frac{\partial V_i}{\partial x_i} = 0 \tag{4}$$

$$\rho\frac{\partial (V_i V_j)}{\partial x_i} = \frac{\partial}{\partial x_i}\left(\mu\frac{\partial V_j}{\partial x_i}\right) - \frac{\partial p}{\partial x_i} \tag{5}$$

$$\rho\frac{\partial (V_i c_p T)}{\partial x_i} = \frac{\partial}{\partial x_i}\left(\lambda\frac{\partial T}{\partial x_i}\right) \tag{6}$$

As shown in Fig. 2, the flow emanates from the center of the disk to the point at the perimeter of the disk. The related boundary conditions are described as follows:

- Inlet: mass flow of water ($\dot{m}$), the mass flow is 1 g/s for each central channel. Note that the corresponding Reynolds number is around 40 at inlet and the Knudsen number is about 0.0015.
- Outlet: pressure outlet. The reference pressure (atmosphere pressure) is specified at this boundary.
- Interface: As compared to the outer heat sink and chip, channels are of smaller scales. To ensure accuracy of simulation in the channels and control the total number of grids, we need to use two-level grids with different size steps for the channels and the outer part. To connect the two parts, a conjugate interface between the channels and outer walls was selected.
- Along the top wall of the sink: a constant heat flux of $q_0'' = 10$ W/cm$^2$ is applied; Other walls are specified to be adiabatic.

Grid-independence of the final results was checked for each geometrical configuration by analysis of pressure distribution of four designs of the mesh with different grid densities. The comparison results show that the difference of pressure drop between the $12 \times 12 \times$mod and $16 \times 16 \times$mod is only 0.7%. Therefore, the final grid system used here is about $16 \times 16 \times$mod ($l_k$/0.1 mm) for each channel segment. For the outer domain (chip and heat sink), a size step of 2.0 mm for the $x$- and $y$- directions and 24 mesh grids in the $z$- direction were used. The total number of grids was around one million for all of the designed geometries tested. A second upwind discretization scheme was used considering the stability of solution convergence. The SIMPLEC algorithm was employed for the pressure-velocity coupling. The convergence criteria for the residual is $1 \times 10^{-5}$ for all the equations except for $1 \times 10^{-8}$ for the energy equation.

**Table 2**
Channel dimensions of tree-like networks ($m = 3$). $R = 20$. (unit: mm).

| Case | $h_t$ | $l_0$ | $w_0$ | $l_1$ | $w_1$ | $l_2$ | $w_2$ | $l_3$ | $w_3$ | $A_{in}$ | $A_{tot}$ |
|---|---|---|---|---|---|---|---|---|---|---|---|
| Tree-like (Sym.) | 0.5 | 7.8 | 0.5 | 5.85 | 0.4 | 4.03 | 0.3 | 2.84 | 0.25 | 0.25 | 97 |
| Leaf-like (Sym.) | 0.5 | 20 | 0.5–0.25 | 5.20 | 0.25 | – | – | – | – | 0.25 | 97 |
| Leaf-like (Asym.) | 0.5 | 20 | 0.5–0.25 | 5.20 | 0.25 | – | – | – | – | 0.25 | 97 |

**Table 3**
Properties of liquid (water) and solid.

| | Silicon ($T = 310$ K) | Water ($p = 1$ atm, 273.15 K $\le T \le$ 373.15 K) |
|---|---|---|
| Density $\rho$ (kg/m$^3$) | 2330 | $914.56 + 1.30T - 0.036T^2$ |
| Thermal conductivity $\lambda$ (W/m K) | 125 | $-0.794 + 7.628 \times 10^{-3}T - 9.866 \times 10^{-6}T^2$ |
| Specific heat capacity $c_p$ (J/kg K) | 700 | $1089.03 - 58.15T + 0.166T^2 - 1.55 \times 10^{-4}T^3$ |
| Dynamic viscosity $\mu$ (Pa s) | | $0.458 - 5.29 \times 10^{-3}\,T + 2.30 \times 10^{-5}\,T^2 - 4.45 \times 10^{-8}\,T^3 + 3.24 \times 10^{-11}\,T^4$ |

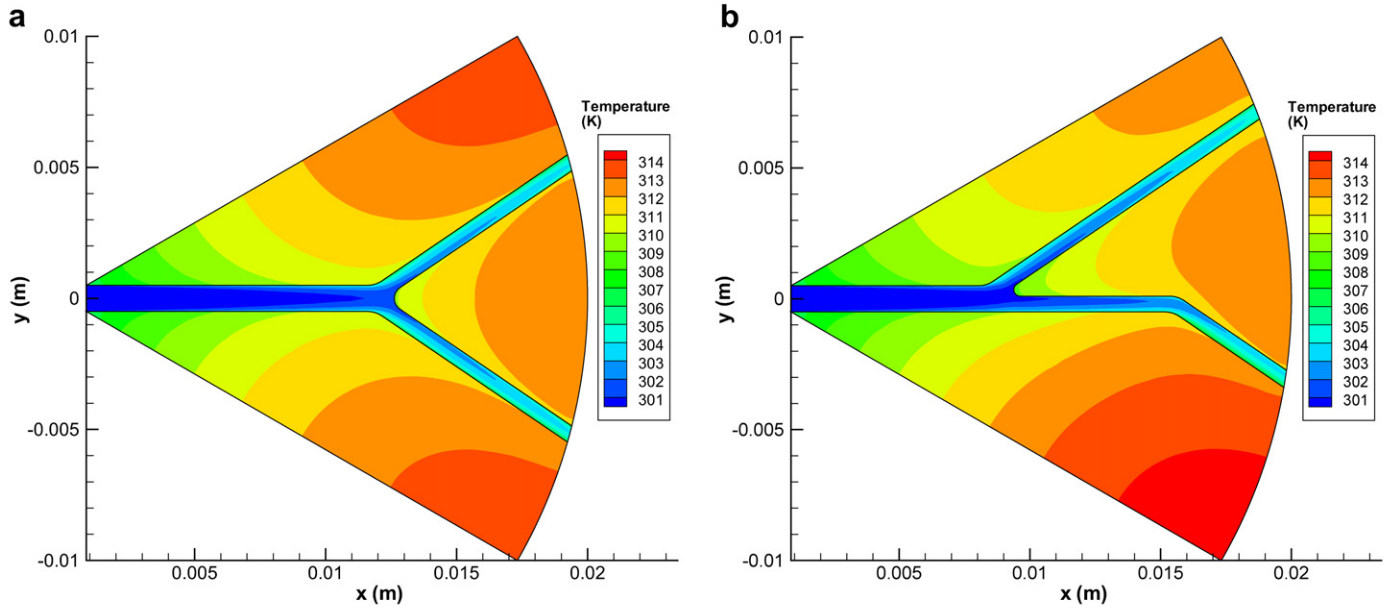


**Fig. 4.** Temperature contours over the middle plane ($z = h_t/2$) of the two tree-like networks: (a) Symmetric tree-like network; (b) Asymmetric tree-like network.

## 3. Results and discussion

### 3.1. Simple network designs (m = 1)

For the simple network design, the computed temperature distributions over the middle plane ($z = h_t/2$) for the symmetric and asymmetric tree-like networks are shown in Fig. 4(a) and (b). It is evident that the temperature contours are similar for the two designs except that for the asymmetric case there is a high temperature region at the bottom corner which is not found in the symmetric case. However, the maximum temperature ($T_{max}$) and the temperature difference ($\Delta T$) are almost the same for the two cases.

Fig. 5 shows velocity contours over the middle plane ($z = h_t/2$) for the two tree-like network. It should be noted that the bifurcations of the channels were streamlined using the fillet technique. It is observed from this figure that there is a stagnation point at the bifurcation, which results in the sharp increase of the local pressure there (Fig. 7). The total pressure drop of the system is thus decreased due to the local pressure recovery [15].

The local heat transfer coefficient ($h' = q''/(T - T_{ref})$) contours on the bottom plane ($z = 0$) for the two networks are displayed in Fig. 6(a) and (b). In general, $h'$ decreases from the inlet to the outlet gradually. However, for the asymmetric network, due to its offset design, the heat transfer coefficient near the top corner is higher than that near the bottom corner (see Fig. 4(b)). The offset deign does not decrease the average heat transfer coefficient for the bottom wall.

We now examine the effect of the asymmetrical design on the static pressure distribution. Fig. 7 shows the pressure distribution

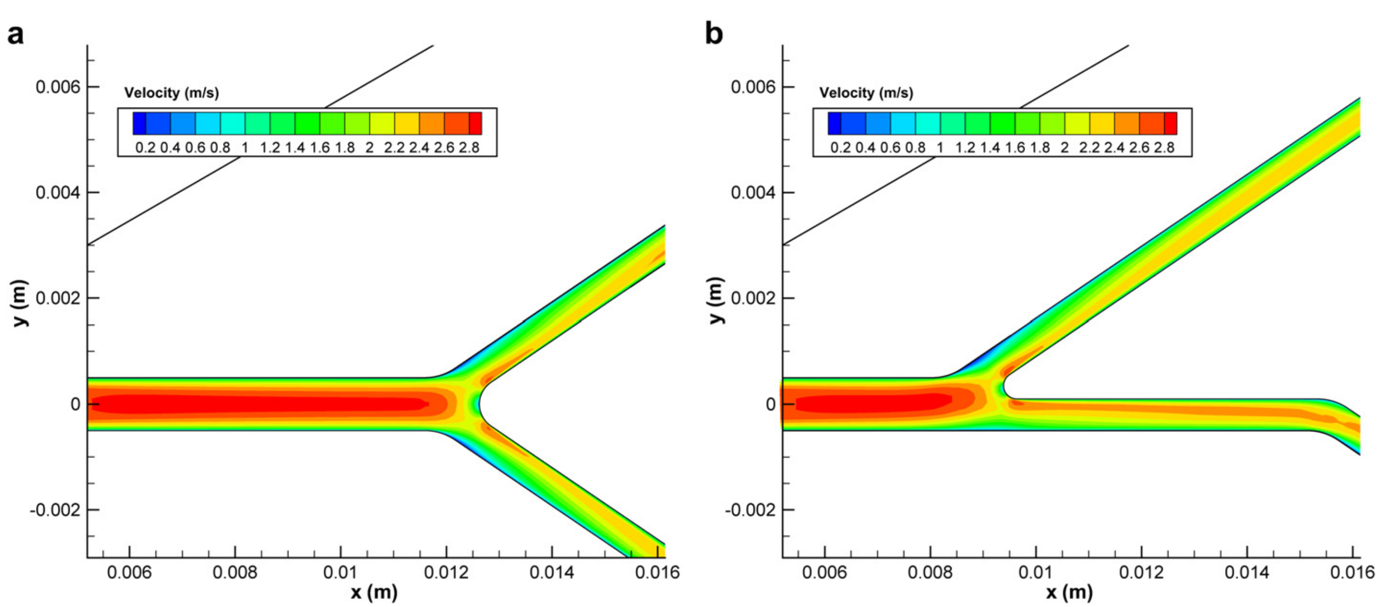


**Fig. 5.** Velocity contours over the middle plane ($z = h_t/2$) of the two tree-like networks: (a) Symmetric tree-like network; (b) Asymmetric tree-like network.

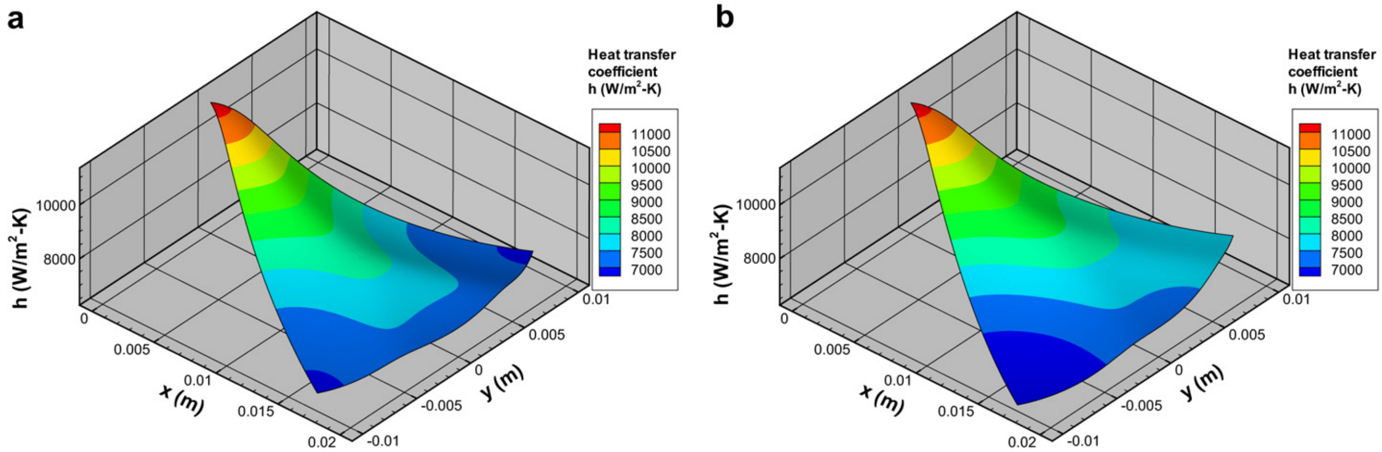


**Fig. 6.** Local heat transfer coefficient contours on the bottom plane ($z = 0$) of the two tree-like networks: (a) Symmetric tree-like network; (b) Asymmetric tree-like network.

along the center-line of the two tree-like networks. The channel segments of the network are represented by three lines (Line-1, Line-2, and Line-3) as shown in this figure. For the symmetric case, Line-2 and Line-3 overlap since the pressure distribution is identical. For the asymmetric case, Line-2 first deviates from the main channel, followed by Line-3. It is found from this figure that the pressure drop for the asymmetric case is a little lower than that of the symmetric case. Although the magnitude is not appreciable, it is worth further study. Investigation of high-level branching networks is necessary for clarification of these observations.

### 3.2. Complex network designs (m = 3)

A rectangular heat sink ($L = 20$ mm, $H = 9$ mm) was used for ease of design and simulation. For comparison, three geometries were selected as shown in Fig. 3: symmetric tree-like network, symmetric leaf-like network, and asymmetric leaf-like network. The latter two net designs mimic the natural leaf structure as shown in Fig. 1 without the lower-level loops between the side branches. Since such a structure is found in natural systems, this may offer some advantages which deserve further study.

Fig. 8 shows the computed temperature distribution over the middle plane ($z = h_t/2$) for the three network. It is observed that the tree-like network presents the highest maximum temperature ($T_{max} = 309.97$ K), followed by the asymmetrical leaf-like network ($T_{max} = 309.25$ K) and the symmetric leaf-like network ($T_{max} = 308.51$ K). Although the difference in the maximum temperature is relatively small, the contour distribution is quite different from each other. As can be seen from the figures, the tree-like network cannot adequately cover the region near the inlet, hence the sink temperature near this part is relatively high. However, for the leaf-like networks, the channel segments are distributed more uniformly as compared to the tree-like network, so the sink temperature increases from the left side to the right side (similar to what happens in the parallel straight channel networks).

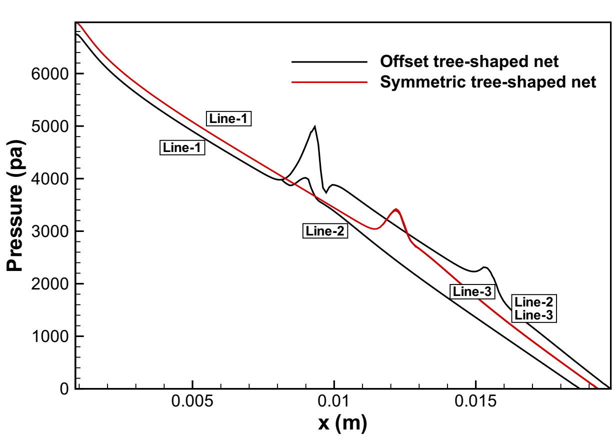


**Fig. 7.** Pressure distribution along the center-line of the two tree-like networks.

The velocity distributions over the middle plane ($z = h_t/2$) for the three networks are shown in Fig. 9(a)–(c). It is seen from this figure and Table 4 that the velocity distribution in each channel segment is not uniform in all three cases. It should be noted that in Table 4 only half of the outlets are listed for the symmetric tree-like and leaf-like networks due to symmetric conditions. For the symmetric tree-like network, Outlet-1 and Outlet-8 (as labeled in Fig. 3) have the highest velocities since the fluid takes the path of least resistance. Similarly, for the symmetric leaf-like network, the outlet of the main channel (Outlet-0) has the highest velocity, followed by the side channels from left to right side. With respect to the velocity distributions, the bulk temperature of the outlets demonstrates similar distributions, as shown in Table 4.

Fig. 10(a)–(c) displays the local heat transfer coefficient ($h'$) distributions over the bottom wall for the three types of branching networks. It is clearly seen that the leaf-like networks have higher average heat transfer coefficient as compared to the tree-like network. This means this design of a tree-like network is not suitable for a rectangular chip cooling application. However, the leaf-like networks show some advantages considering the temperature and heat transfer distributions. As compared to the asymmetric leaf-like network, the average heat transfer coefficient of the symmetric network is relatively higher, although the difference is small for the parameters studied.

Fig. 11 shows possibly the most interesting phenomenon with leaf-shaped designs; they decrease the total pressure drop appreciably. From this figure, it can be observed that the pressure drop of the leaf-like network is only about half that of the symmetric tree-like network (without offset). Between the two leaf-like networks, the asymmetrical network has a lower pressure drop than the symmetrical one. The side channels of the leaf-like networks act as "buffers" to recover the local pressure distribution. Hence the total pressure drop is reduced by the presence of multiple bifurcations (or "buffers"). Actually, the pressure recovery is the essentially result of the geometrical configuration at the bifurcation of the flow network, which has also been found in fractal-like channel

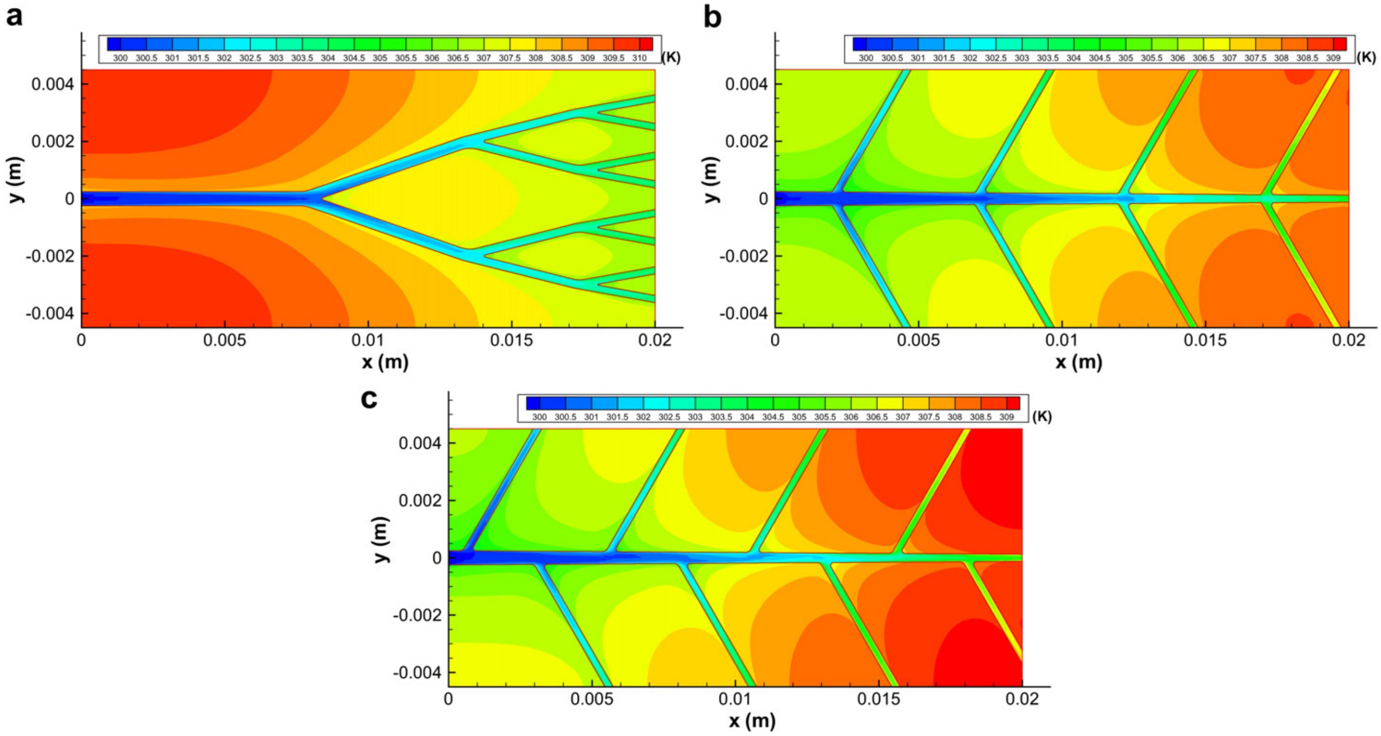


**Fig. 8.** Temperature distributions over the middle plane ($z = h_t/2$) for three types of networks: (a) Symmetric tree-like network; (b) Symmetric leaf-like network; (c) Asymmetric/Offset leaf-like network.

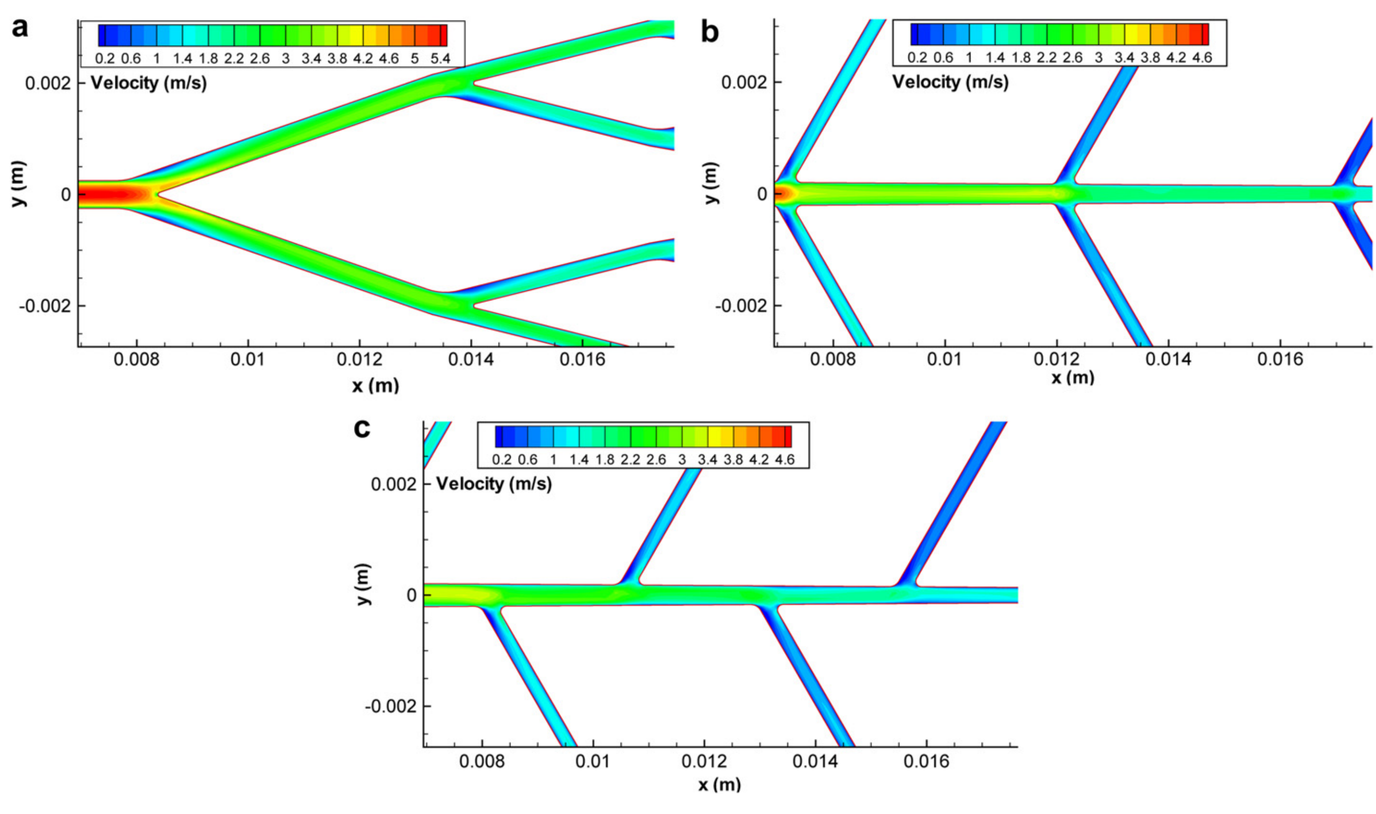


**Fig. 9.** Velocity distributions over the middle plane ($z = h_t/2$) for three types of networks: (a) Symmetric tree-like network; (b) Symmetric leaf-like network; (c) Asymmetric/Offset leaf-like network.

**Table 4**
Velocity and temperature at the outlets for the three networks.

| Case | Outlet | Velocity (m/s) | | | | | Temperature (K) | | | | |
|---|---|---|---|---|---|---|---|---|---|---|---|
| | | 0 | 1 | 2 | 3 | 4 | 0 | 1 | 2 | 3 | 4 |
| Tree-like (Sym.) | – | 1.14 | 0.88 | 0.73 | 0.91 | – | 304.35 | 304.60 | 304.84 | 304.63 | |
| Leaf-like (Sym.) | 0.95 | 0.88 | 0.67 | 0.50 | 0.24 | 305.25 | 303.81 | 304.85 | 306.11 | 307.62 | |
| Leaf-like (Asym.) | 0.65 | 1.35 | 0.78 | 0.58 | 0.33 | 306.22 | 302.83 | 304.57 | 305.98 | 307.75 | |
| | | | 5 | 6 | 7 | 8 | | 5 | 6 | 7 | 8 |
| | | | 0.21 | 0.47 | 0.69 | 0.90 | | 308.21 | 306.84 | 305.21 | 304.07 |

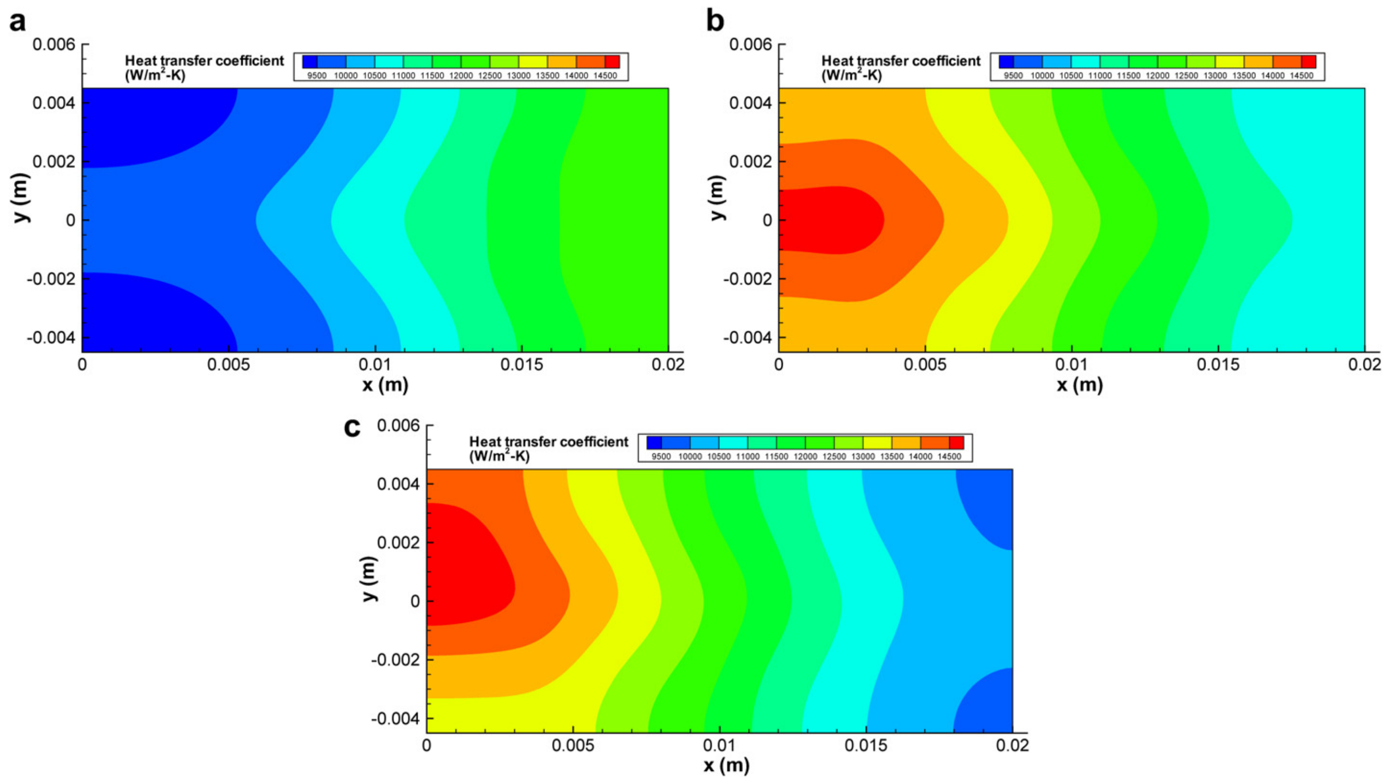


**Fig. 10.** Heat transfer coefficient distribution over the bottom wall ($z = 0$) for three types of networks: (a) Symmetric tree-like network; (b) Symmetric leaf-like network; (c) Asymmetric/Offset leaf-like network.

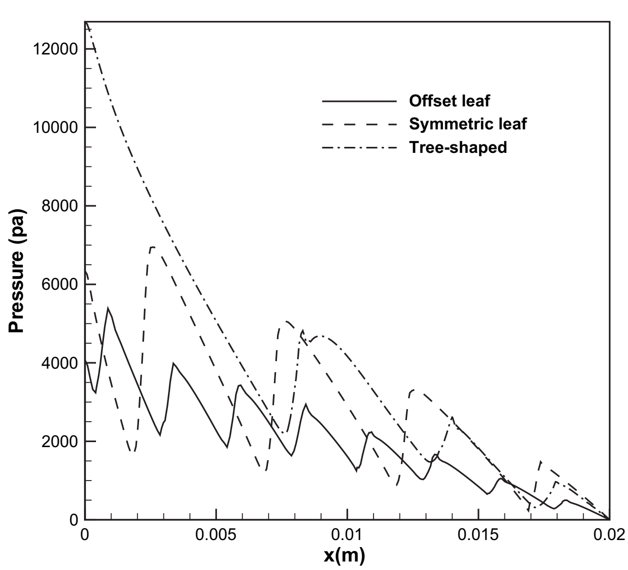


**Fig. 11.** Pressure distribution along the center-line of the three networks.

networks by Alharbi et al. [31,32]. For the asymmetric network, the increased number of "buffers" shows the best performance in decreasing the pressure drop. However, for the symmetric network, the number of "buffers" is only half, hence it has a higher pressure drop as compared to the symmetrical network.

Considering the balance between the pressure drop and the heat transfer performance, we cannot draw definitive conclusions as to which leaf-like network is better than the other. The symmetrical network has a relatively higher pressure drop and lower heat transfer coefficient. But for the asymmetrical network, the converse is true. This may explain why both networks co-exist in nature.

## 4. Conclusion

The present study focused on a comparison between the symmetrical and asymmetrical (or offset) branching networks built into heat sinks considering their fluid flow and heat transfer characteristics. For the simplest design ($m = 1$), the differences relatively small. However, when comparing the symmetrical tree-like network and the symmetrical/asymmetrical leaf-like networks, the difference is obvious, especially in the pressure distribution and pressure drop. Results show the advantages of the leaf-like networks.

As compared to the tree-like networks with high branching levels, such leaf-like networks seem much simpler and show better thermal performance. However, due to the simplifications made in this work, further investigations are needed. For example, to improve the temperature uniformity, optimization of the side channels should be evaluated. Also, for the real leaf systems, the loops between the side channels probably play an important role in the transport process; the effect of loops needs to be investigated for offset network designs.

## References

[1] G.B. West, J.H. Brown, B.J. Enquist, A general model for the origin of allometric scaling laws in biology, Science 276 (1997) 122–126.

[2] A. Bejan, Shape and Structure, from Engineering to Nature, Cambridge University Press, Cambridge, 2000.

[3] D.V. Pence, Improved thermal efficiency and temperature uniformity using fractal-like branching channel networks, in: Proceedings of the International Conference on Heat Transfer and Transport Phenomena in Micro Scale, Banff, Canada, 2000, pp. 142–148.

[4] Y. Chen, P. Cheng, Heat transfer and pressure drop in fractal tree-like microchanel nets, Int. J. Heat Mass Transfer 45 (2002) 2643–2648.

[5] K.A. McCulloh, J.S. Sperry, F.R. Adler, Water transport in plants obeys Murray's law, Nature (London) 421 (2003) 939–942.

[6] B. Mauroy, M. Filoche, E.R. Weibel, et al., An optimal bronchial tree may be dangerous, Nature (London) 427 (2004) 633–636.

[7] S.M. Senn, D. Poulikakos, Tree network channels as fluid distributors constructing double-staircase polymer electrolyte fuel cells, J. Appl. Phys. 96 (2004) 842–852.

[8] D. Tondeur, L. Luo, Design and scaling laws of ramified fluid distributors by constructal approach, Chem. Eng. Sci. 59 (2004) 1799–1813.

[9] D.R. Emerson, K. Cieślicki, X. Gu, et al., Biomimetic design of microfluidic manifolds based on a generalized Murray's law, Lab. Chip 6 (2006) 447–454.

[10] D.V. Pence, Reduced pumping power and wall temperature in microchannel heat sinks with fractal-like branching channel networks, Microscale Thermophys. Eng. 6 (2002) 319–330.

[11] D.V. Pence, K.E. Enfield, Inherent benefits in microscale fractal-like devices for enhanced transport phenomena, in: M. Collins, C.A. Brebbia (Eds.), Design and Nature, WIT Press, Rhodes, Greece, 2004, pp. 317–328.

[12] S.M. Senn, D. Poulikakos, Laminar mixing, heat transfer and pressure drop in tree-like microchannel nets and their application for thermal management in polymer electrolyte fuel cells, J. Power Sources 130 (2004) 178–191.

[13] Y. Chen, P. Cheng, An experimental investigation on the thermal efficiency of fractal tree-like microchannel nets, Int. Commun. Heat Mass Transfer 32 (2005) 931–938.

[14] Xiang-Qi Wang, Arun S.Mujumdar, Christopher Yap, Thermal characteristics of tree-shaped microchannel nets for cooling of a rectangular heat sink, Int. J. Therm. Sci. 45 (2006) 1103–1112.

[15] Xiang-Qi Wang, Arun S. Mujumdar, Christopher Yap, Numerical analysis of blockage and optimization of heat transfer performance of fractal-like microchannel nets, J. Electron. Packag 128 (2006) 38–45.

[16] Xiang-Qi Wang, Arun S. Mujumdar, Christopher Yap, Effect of bifurcation angle in tree-shaped microchannel networks, J. Appl. Phys. 102 (2007) 073530.

[17] D.B. Tuckerman, R.F.W. Pease, High-performance heat sinking for vlsi, IEEE Electron Device Lett. EDI-2 (5) (1981) 126–129.

[18] H.H. Bau, Optimization of conduits' shape in micro heat exchangers, Int. J. Heat Mass Transfer 41 (1998) 2717–2723.

[19] V.D. Zimparov, A.K. da Silva, A. Bejan, Thermodynamic optimization of tree-shaped flow geometries with constant channel wall temperature, Int. J. Heat Mass Transfer 49 (2006) 4839–4849.

[20] V.D. Zimparov, A.K. da Silva, A. Bejan, Constructal tree-shaped parallel flow heat exchangers, Int. J. Heat Mass Transfer 49 (2006) 4558–4566.

[21] C. Biserni, L.A.O. Rocha, G. Stanescu, E. Lorenzini, Constructal H-shaped cavities according to Bejan's theory, Int. J. Heat Mass Transfer 50 (2007) 2132–2138.

[22] T. Bello-Ochende, A. Bejan, Constructal multi-scale cylinders in cross-flow, Int. J. Heat Mass Transfer 48 (2005) 1373–1383.

[23] T. Bello-Ochende, L. Liebenberg, J.P. Meyer, Constructal cooling channels for micro-channel heat sinks, Int. J. Heat Mass Transfer 50 (2007) 4141–4150.

[24] T. Bello-Ochende, L. Liebenberg, J.P. Meyer, Constructal design: geometric optimization of micro-channel heat sinks, SA J. Sci. 103 (2007) 483–489.

[25] C.D. Murray, The physiological principle of minimum work. I. The vascular system and the cost of blood volume, Proc. Natl. Acad. Sci. U.S.A. 12 (1926) 207–214.

[26] H.B.M. Uylings, Optimization of diameters and bifurcation angles in lung and vascular tree structures, Bull. Math. Biol. 39 (1977) 509–519.

[27] T.F. Sherman, On connecting large vessels to small – the meaning of Murray's law, J. Gen. Physiol. 78 (1981) 431–453.

[28] A. Bejan, L.A.O. Rocha, S. Lorente, Thermodynamic optimization of geometry: T- and Y-shaped constructs of fluid steams, Int. J. Therm. Sci. 39 (2000) 949–960.

[29] H. Zhang, S. Lorente, A. Bejan, Vascularization with trees that alternate with upside-down trees, J. Appl. Phys. 101 (2007) 094904.

[30] W. Wechsatol, S. Lorente, A. Bejan, Optimal tree-shaped networks for fluid flow in a disc-shaped body, Int. J. Heat Mass Transfer 45 (2002) 4911–4924.

[31] A.Y. Alharbi, D.V. Pence, R.N. Cullion, Fluid flow through microscale fractal-like branching channel networks, J. Fluids Eng. Trans. ASME 125 (2003) 1051–1057.

[32] A.Y. Alharbi, D.V. Pence, R.N. Cullion, Thermal characteristics of microscale fractal-like branching channels, J. Heat Transf. Trans. ASME 126 (2004) 744–752.